The Journal of Immunology

Differential Features of AIRE-Induced and AIRE-Independent Promiscuous Gene Expression in Thymic Epithelial Cells

Charles St-Pierre, Assya Trofimov, Sylvie Brochu, Sébastien Lemieux and Claude Perreault

J Immunol 2015; 195:498-506; Prepublished online 1 June 2015;
doi: 10.4049/jimmunol.1500558
http://www.jimmunol.org/content/195/2/498

The Journal of Immunology is published twice each month by
The American Association of Immunologists, Inc.,
1451 Rockville Pike, Suite 650, Rockville, MD 20852

Print ISSN: 0022-1767 Online ISSN: 1550-6606.

Differential Features of AIRE-Induced and AIRE-Independent Promiscuous Gene Expression in Thymic Epithelial Cells

Charles St-Pierre,*,† Assya Trofimov,*,†,‡ Sylvie Brochu,*,† Sébastien Lemieux,*,‡ and Claude Perreault*,†

Establishment of self-tolerance in the thymus depends on promiscuous expression of tissue-restricted Ags (TRA) by thymic epithelial cells (TEC). This promiscuous gene expression (pGE) is regulated in part by the autoimmune regulator (AIRE). To evaluate the commonalities and discrepancies between AIRE-dependent and -independent pGE, we analyzed the transcriptome of the three main TEC subsets in wild-type and *Aire* knockout mice. We found that the impact of AIRE-dependent pGE is not limited to generation of TRA. AIRE decreases, via non–cell autonomous mechanisms, the expression of genes coding for positive regulators of cell proliferation, and it thereby reduces the number of cortical TEC. In mature medullary TEC, AIRE-driven pGE upregulates non-TRA coding genes that enhance cell–cell interactions (e.g., claudins, integrins, and selectins) and are probably of prime relevance to tolerance induction. We also found that AIRE-dependent and -independent TRA present several distinctive features. In particular, relative to AIRE-induced TRA, AIRE-independent TRA are more numerous and show greater splicing complexity. Furthermore, we report that AIRE-dependent versus -independent TRA project nonredundant representations of peripheral tissues in the thymus. ***The Journal of Immunology*****, 2015, 195: 498–506.**

In all gnathostomes, thymic function and architecture are remarkably conserved and the thymus is the sole organ able to produce classic T cells (1, 2). Although the thymic cortex is necessary for thymocyte expansion and positive selection, the primary role of the thymic medulla is in the generation of self-tolerance via negative selection and the generation of regulatory T cells (3–5). Failure to establish or maintain self-tolerance causes autoimmunity, which has a major impact on human health. Classic autoimmune diseases such as rheumatoid arthritis, type 1 diabetes, and multiple sclerosis affect ∼4% of the general population (6). Induction of so-called "central tolerance" in the thymic medulla depends on ectopic expression of proteins otherwise restricted to differentiated organs in the periphery (7). Remarkably, the medullary thymic epithelial cell (mTEC) population collectively expresses almost the entire repertoire of known protein-coding genes (8, 9) and can therefore induce tolerance to a wide array of tissue-restricted Ags (TRA). Promiscuous gene expression (pGE) by mTEC is essential to induce tolerance to protein whose expression otherwise would be strictly extrathymic.

Although pGE evolved as a fascinating strategy for enhancing the scope of self-tolerance, the mechanisms underpinning this crucial process are still poorly defined. To date, the only known molecular determinant driving pGE in the thymus is the autoimmune regulator (AIRE), a transcriptional regulator that does not act as a conventional transcription factor (10–12). AIRE interacts with repressive epigenetic marks and recruits proteins that promote transcriptional elongation and pre-mRNA processing (13, 14). In addition to its role in promoting the expression of TRA for the purpose of negative selection (10), AIRE also affects mTEC development (15), enhances Ag presentation to thymocytes (16), and regulates Ag transfer from mTEC to dendritic cells (DCs) (17). However, the molecular mechanisms underlying these effects are still unknown. Furthermore, AIRE regulates the pGE of only a fraction of TRA (18). The identity of transcriptional regulators driving AIRE-independent pGE and their functional significance remains elusive.

The goal of our work was therefore to address two questions. First, irrespective of its role in the generation of TRA, how might AIRE affect TEC function? Second, what are the commonalities and discrepancies between AIRE-dependent and -independent pGE? To this end, we used high-throughput RNA sequencing (RNA-seq) to analyze the poly(A)$^+$ transcriptome of the three main TEC populations in wild-type (WT) and *Aire* knockout (KO) mice. We found that AIRE has pervasive effects not only on mTEC but also on cortical TEC (cTEC) biology. Furthermore, we report that AIRE-dependent versus -independent TRA present several differential features and project nonredundant representations of peripheral tissues in the thymus.

*Institute for Research in Immunology and Cancer, University of Montreal, Montreal, Quebec H3C 3J7, Canada; †Department of Medicine, University of Montreal, Montreal, Quebec H3C 3J7, Canada; and ‡Department of Computer Science and Operations Research, University of Montreal, Montreal, Quebec H3C 3J7, Canada

ORCID: 0000-0001-9453-7383 (C.P.).

Received for publication March 9, 2015. Accepted for publication May 4, 2015.

This work was supported by Canadian Institute of Health Research Grant MOP 42384. C.S.-P. is supported by a doctoral scholarship from Le Fonds de Recherche du Québec–Santé and C.P. holds a Canada Research Chair in immunobiology. The Institute for Research in Immunology and Cancer is supported in part by the Canada Foundation for Innovation and the Fonds de la Recherche en Santé du Québec.

The RNA-seq data presented in this article have been submitted to the Gene Expression Omnibus under accession number GSE65617.

Address correspondence and reprint requests to Prof. Claude Perreault, Institute for Research in Immunology and Cancer, P.O. Box 6128, Station Centre-Ville, Montreal, QC H3C 3J7, Canada. E-mail address: claude.perreault@umontreal.ca

The online version of this article contains supplemental material.

Abbreviations used in this article: AIRE, autoimmune regulator; APECED, autoimmune polyendocrinopathy–candidiasis–ectodermal dystrophy; CE, cornified envelope; cTEC, cortical thymic epithelial cell; DC, dendritic cell; DEG, differentially expressed gene; ESC, embryonic stem cell; GO, gene ontology; KO, knockout; MHC II, MHC class II; mTEC, medullary thymic epithelial cell; *p-adj*, adjusted *p*; pGE, promiscuous gene expression; RNA-seq, RNA sequencing; RPKM, reads per kb per million reads; SPRR, small proline-rich; TEC, thymic epithelial cell; TRA, tissue-restricted Ag; UEA1, *Ulex europaeus* lectin 1; WT, wild-type.

Materials and Methods

Mice

B6.129S2-*Aire*$^{tm1.1Doi}$/J mice were purchased from The Jackson Laboratory (Bar Harbor, ME). Heterozygous mice (*Aire*$^{+/-}$) were mated and 6- to 8-wk-old homozygous littermates (*Aire*$^{+/+}$ and *Aire*$^{-/-}$ mice) were used in all experiments. B6.129S2-*Aire*$^{tm1.1Doi}$/J mice were bred and housed under specific pathogen-free conditions in sterile ventilated racks at the Institute for Research in Immunology and Cancer. All procedures were in accordance with the Canadian Council on Animal Care guidelines and approved by the Comité de Déontologie et Expérimentation Animale de l'Université de Montréal.

Flow cytometry analyses and cell sorting

Thymi were isolated and stromal cell enrichment was performed as described (19). In brief, thymi were mechanically disrupted and digested with DNase I (Sigma-Aldrich) and Liberase (Roche). Thymic stromal cells were either further enriched using anti-CD45 Microbeads (Miltenyi Biotec) or stained directly with biotinylated *Ulex europaeus* lectin 1 (UEA1; Vector Laboratories), PE-Cy7–conjugated streptavidin (BD Biosciences), and the following Ab: Alexa Fluor 700 anti-CD45, PE anti–I-A^b, FITC anti-CD80 (BD Biosciences), allophycocyanin-Cy7 anti-EpCAM, and Alexa Fluor 647 anti-Ly51 (BioLegend). Cell viability was assessed using 7-aminoactinomycin D (BD Biosciences). Isolation of TEC subsets was performed as previously described (8, 20). Live TEC were selected as 7-aminoactinomycin D$^-$ CD45$^-$EpCAM$^+$ and sorted as cTEC (Ly51$^+$UEA1$^-$), mTEC^{lo} (Ly51$^-$ UEA1$^+$CD80^{lo}MHC class II[MHC II]^{lo}), and mTEC^{hi} (Ly51$^-$UEA1$^+$CD80^{hi} MHC II^{hi}). For intracellular staining, cell viability was assessed using the Live/Dead fixable blue dead cell stain kit (Invitrogen) and cells were fixed/permeabilized using the Foxp3 staining buffer Set (eBioscience) and stained with eFluor 660 anti-AIRE Ab (eBioscience). TEC were sorted on a three-laser FACSAria (BD Biosciences) or analyzed on a three-laser LSR II (BD Biosciences) using FACSDiva software.

RNA extraction and cDNA libraries preparation

Total RNA was isolated using TRIzol as recommended by the manufacturer (Invitrogen), and then further purified using the RNeasy micro kit (Qiagen). Sample quality was assessed using Bioanalyzer RNA Pico chips (Agilent Technologies). A minimum of 10,000 cells were used for the RNA-seq experiment (average of 20,000 cells), yielding an average of ~20 ng total RNA. Transcriptome libraries were generated from total extracted RNA using the TruSeq RNA sample prep kit (v2) (Illumina) following the manufacturer's protocols.

RNA-seq

RNA-seq was performed as described (8). Briefly, paired-end (2 × 100 bp) sequencing was performed using the Illumina HiSeq 2000 machine running TruSeq v3 chemistry. Three RNA-seq libraries were sequenced per lane (eight lanes per slide). Details of the Illumina sequencing technologies can be found at http://www.illumina.com/applications/sequencing/rna.html. Data were mapped to the *Mus musculus* (mm10) reference genome using the ELANDv2 alignment tool from the CASAVA 1.8.2 software or TopHat/Cufflinks 2.2.1 for analyses at the isoform transcript level. Keeping only uniquely matching reads, we used the read count per transcript for the identification of differentially expressed genes. We then used the statistical method based on a negative binomial distribution and implemented in the DESeq package for R to compare samples and obtain a robust measure of differential expression between samples (21, 22). The resulting *p* values were adjusted for multiple testing with the Benjamin–Hochberg procedure to yield *p-adj* values. To estimate gene expression, we quantified transcript levels as reads per kb of exon model per million mapped reads (RPKM) (23). RNA-seq data have been deposited in Gene Expression Omnibus archives under accession number GSE65617.

Gene ontology analyses

Input gene datasets were tabulated and uploaded into the bioinformatics resource DAVID v6.7. This online tool was used to assess the enrichment of input genes with gene ontology (GO) biological process terms (24, 25). We used all genes of the mouse genome as background and considered a *p* value of <0.05 to be significant. Only nonredundant biological processes with significant enrichment were investigated.

Statistical and bioinformatics analyses

Statistical tests and bioinformatics analyses were done using R version 3.1.0 or Excel version 14.4.7. Unless stated otherwise, data are represented as mean ± SD. Statistical significance was assessed by a two-tailed Student *t* test unless stated differently and differences with a p value < 0.05 were considered significant. Splicing complexity was measured by the Shannon entropy of the relative isoform abundances of genes with more than one detectable isoform. Splicing complexity was calculated for each gene as:

$$\sum_{i=1}^{n} P_i \log_2(P_i),$$

where n is the number of detectable isoforms per gene and P is the proportion contribution of each isoform i to total gene expression. Genes with no complexity have a single detectable isoform whereas genes with equally abundant isoforms have maximal complexity.

Results

Dynamics of TEC populations in WT and Aire*-deficient mice*

As a prelude to transcriptomic analyses, we assessed the size of the main TEC subsets in 6- to 8-wk-old WT and *Aire*$^{-/-}$ littermates. TEC (EpCAM$^+$CD45$^-$) were defined as cTEC and mTEC based on the expression of Ly51 and binding of the UEA1 lectin (8, 20). mTEC were further divided into mTEC^{lo} and mTEC^{hi} based on low or high expression of CD80 and MHC II molecules (Fig. 1A, Supplemental Fig. 1).

Aire is expressed strictly in mTEC^{hi} (26) and modulates mTEC differentiation (15). In accordance with this, we observed that, relative to their WT littermates, *Aire*-KO mice displayed a significant increase in the absolute number of mTEC^{hi} whereas the number of mTEC^{lo} remained unchanged (Fig. 1B, Supplemental Fig. 2). Consequently, the proportion of mTEC^{lo} and mTEC^{hi} was also severely altered in KO mice (Fig. 1C). Nonetheless, the unexpected finding was a 1.6-fold increase in the absolute number of cTEC in KO mice (Fig. 1B). AIRE's impact on cTEC number is non–cell autonomous because cTEC do not express the AIRE protein (26).

AIRE has non–cell autonomous effects on the cTEC transcriptome

We performed RNA-seq analyses on three biological replicates for each cell type. Each replicate contained pooled FACS-sorted TEC from four (two males plus two females) 6- to 8-wk-old WT or *Aire* knockout littermates (Fig. 2A). The purity of sorted TEC subsets was >97% (Fig. 2B). To further validate the purity of the sorted primary TEC populations, we confirmed that they expressed expected markers of cTEC and mTEC (Fig. 2C). Note that *Aire* was also detected in *Aire*$^{-/-}$ mice, because only exon 2 and portions of introns 1 and 3 are excised in B6.129S2-*Aire*$^{tm1.1Doi}$/J mice.

To gain insights into the impact of AIRE on cTEC, we compared the transcriptome of FACS-purified WT versus KO cTEC. For analysis of differentially expressed genes (DEGs), we used the *R* package DESeq (21) together with stringent criteria: a fold difference of ≥5 between WT and KO and a *p-adj* < 0.05. We identified a total of 309 genes that were upregulated in KO cTEC whereas only 9 were upregulated in WT cTEC (Fig. 3A). Of note, it is formally possible that gene expression changes in *Aire*-KO cTEC reflect a subset-specific gene upregulation, which cannot be distinguished with bulk RNA-seq. Addressing this issue in future studies would therefore require single-cell approaches. To better characterize the set of genes modulated by AIRE in cTEC, we performed a GO term enrichment analysis on genes overexpressed in KO cTEC that showed a minimum of 1 RPKM (215 out of 309 genes). Genes overexpressed in KO cTEC were associated with 10 main biological processes (Fig. 3B). We analyzed more in depth the three biological processes associated with the highest number of DEGs: epithelial cell differentiation, defense response, and regulation of cell proliferation. The most significantly enriched term in

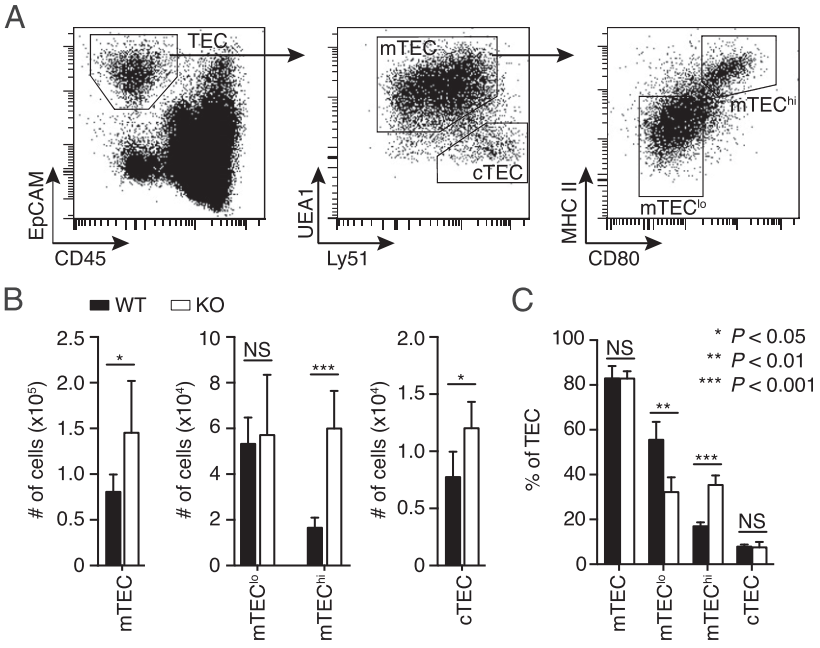

FIGURE 1. Flow cytometry analysis of TEC population in WT and *Aire*-deficient mice. (**A**) Representative flow cytometry profiles with gating strategy for TEC subsets are shown. TEC were defined as $CD45^{-}EpCAM^{+}$ and further divided into cTEC ($Ly51^{+}UEA1^{-}$) and mTEC ($Ly51^{-}UEA1^{+}$). Immature and mature mTEC ($mTEC^{lo}$ and $mTEC^{hi}$) were discriminated based on low or high expression of CD80 and MHC II molecules. (**B**) Absolute cell number and (**C**) proportion of TEC subsets in WT and *Aire*-KO mice. Each group includes four to six mice (two independent experiments). Error bars indicate SD, and asterisks represent the *p* values calculated using a two-tailed Student *t* test.

our gene list was epithelial cell differentiation. Of particular relevance, we found that several genes encoding small proline-rich (SPRR) proteins, including *Sprr1a*, *Sprr2d*, *Sprr2j-ps*, and *Sprr4*, were upregulated in KO cTEC as compared with WT littermates. The *Sprr* multigene family is instrumental in the formation of a cornified envelope (CE), which serves as a protective barrier in various stratified squamous epithelia (27). Moreover, we observed that genes encoding CE structural proteins, including involucrin, cornifelin, and cytokeratin 4, were also upregulated in KO cTEC (28, 29). Taken together, these results suggest that $Aire^{-/-}$ cTEC acquire a more differentiated phenotype by upregulation of genes involved in CE formation.

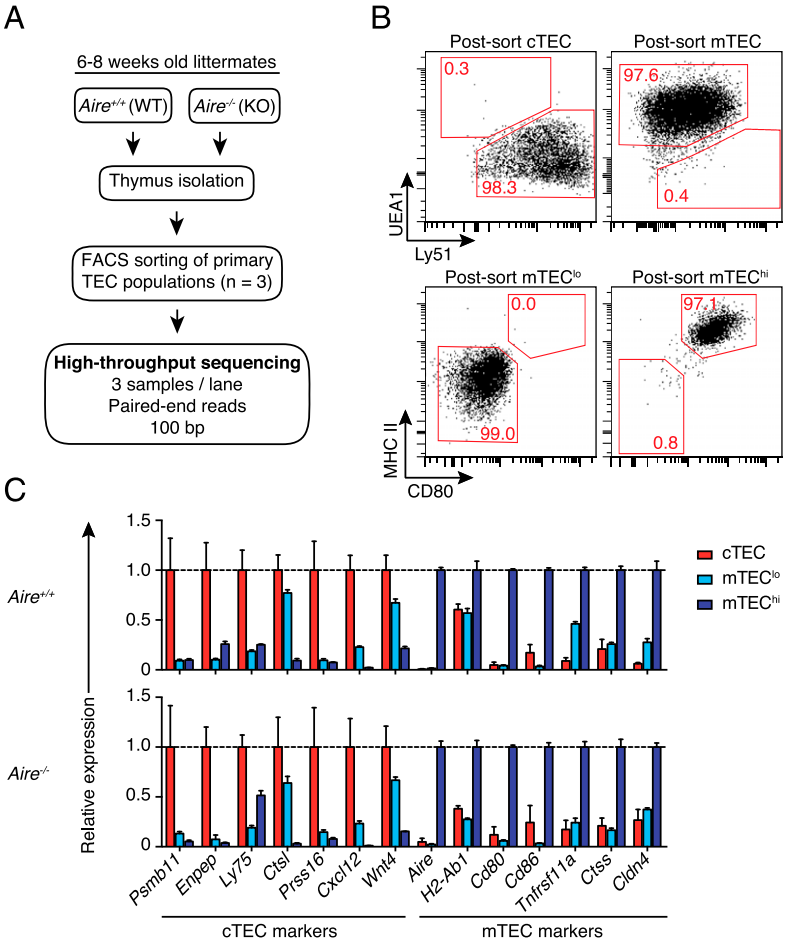

FIGURE 2. RNA-seq of primary cTEC, $mTEC^{lo}$, and $mTEC^{hi}$ harvested from WT and *Aire*-deficient mice. (**A**) RNA-seq study design. (**B**) Postsorting purity of sorted TEC populations. (**C**) Relative mRNA expression of cTEC lineage-specific genes (normalized to cTEC) and mTEC lineage-specific genes (normalized to $mTEC^{hi}$) in WT and KO mice.

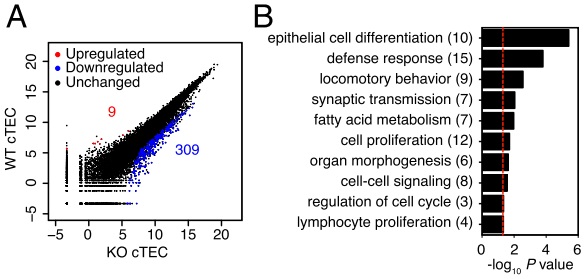

FIGURE 3. Transcriptome of WT and *Aire*-KO cTEC. (**A**) Scatter plot representation of gene expression levels in WT and KO cTEC. Data represent the mean of normalized counts. Genes with fold difference ≥ 5 and *p-adj* < 0.05 between WT and KO mice were considered as DEGs (red and blue dots). (**B**) Histogram shows enriched biological processes ($p < 0.05$; red line) linked to DEGs overexpressed in KO cTEC. Numbers in parentheses indicate the number of DEGs per category. GO term enrichment analysis was performed with DAVID bioinformatic tools.

Among DEGs associated to the GO term "defense response," we found several chemokines (*Ccl8*, *Ccl24*) and ILs (*Il10*, *Il23a*, and *Il25*). Whereas *Il23* contributes to TEC regeneration (30), the impact that other DEGs from this group may have on cTEC biology has yet to be elucidated. Finally, we observed that AIRE was predicted to affect cTEC proliferation (Fig. 3B). Notably, the epithelial mitogen (*Epgn*) and homeobox A13 (*Hoxa13*) genes were both upregulated in KO cTEC. Likewise, *Fgf10*, which enhances TEC proliferation (31), was upregulated in KO cTEC. Upregulation of positive regulators of epithelial cell proliferation in *Aire*-KO cTEC (Fig. 3B) is consistent with and provides a plausible mechanistic explanation for the increased numbers of cTEC in $Aire^{-/-}$ mice (Fig. 1B).

Impact of AIRE on pGE

Because individual TRA are expressed in only a fraction of mTEC at any given time (9, 32, 33), we performed our transcriptomic studies at high sequencing depth (average of 134×10^6 mapped reads/sample) to enable robust detection of low abundance transcripts. Hierarchical clustering based on global gene expression levels revealed that WT mTEC^{hi} were distinct from all other TEC populations (Supplemental Fig. 3A). *Aire* deletion significantly reduced the total number of expressed genes (RPKM > 1) in mTEC^{hi} but not in mTEC^{lo} or cTEC (Supplemental Fig. 3B, 3C). In total, 15,137 protein-coding genes were detected in WT mTEC^{hi} whereas 12,684 were detected in KO mTEC^{hi}, similar to what we observed in other TEC populations (12,636 genes). KO mTEC^{hi} fell in a discrete cluster, halfway between WT mTEC^{hi} and other TEC subsets, suggesting that KO mTEC^{hi} retain an AIRE-independent mTEC^{hi} identity (Supplemental Fig. 3A). Finally, both cTEC and mTEC^{lo} from WT and KO mice generated additional clusters, indicative of a lesser impact of *Aire* deletion in these cells.

To identify genes regulated in a cell autonomous manner by AIRE, we analyzed DEGs between WT versus KO mTEC^{hi} (fold difference ≥ 5 and *p-adj* < 0.05). Of a total of 3338 AIRE-regulated genes (Fig. 4A), 3272 genes were upregulated in WT mTEC^{hi} (AIRE induced) whereas only 66 genes were upregulated in KO mTEC^{hi} (AIRE repressed). Two points can be made from these results. First, AIRE almost always acts as a transcriptional activator rather than a repressor in mTEC^{hi}. This is in stark contrast to the non–cell autonomous effect of AIRE on cTEC where the vast majority of DEGs are upregulated in *Aire*-KO relative to WT cTEC (Fig. 3A). Second, AIRE-induced genes include at least ~14% of all mouse genes.

AIRE is not expressed in the mTEC^{lo} subset, which contains most immature "pre-AIRE" cells and a minority of "post-AIRE"

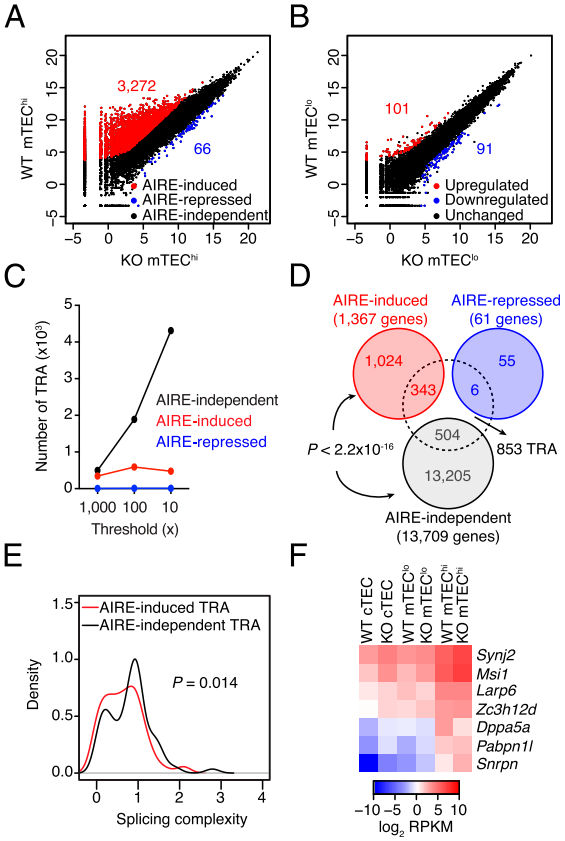

FIGURE 4. The transcriptome of WT versus *Aire*-KO mTEC subsets reveals the breadth of pGE. (**A** and **B**) Transcriptome of WT versus *Aire*-KO (A) mTEC^{hi} and (B) mTEC^{lo}. Genes with fold change ≥ 5 and *p-adj* < 0.05 between WT (*y*-axis) and KO (*x*-axis) were considered as differentially expressed (red and blue dots). Data are represented in a scatter plot as mean of normalized counts. No RPKM threshold was used in these plots. In (**C**)–(**F**), only genes with RPKM of >1 were considered. (C) Number of AIRE-induced (red), AIRE-repressed (blue), and AIRE-independent (black) TRA detected in mTEC^{hi} using various thresholds of tissue-specificity (Supplemental Fig. 4A). (D) Proportion of TRA in AIRE-induced, -repressed, and -independent genes. (E) Splicing complexity of AIRE-induced (red) and AIRE-independent (black) multi-isoform TRA-encoding genes. The Wilcoxon rank sum test was used to statistically assess the difference in splicing complexity. (F) Expression heat map of AIRE-independent mRNA processing factors upregulated in mTEC^{hi} relative to mTEC^{lo} and cTEC.

cells (34). Accordingly, we found only minimal differences between the transcriptome of WT and KO mTEC^{lo} (Fig. 4B). Out of 101 genes overexpressed in WT relative to KO mTEC^{lo}, the vast majority (90 genes) were among the 3272 AIRE-induced genes identified in mTEC^{hi} (data not shown). This is consistent with the notion that post-AIRE mTEC may maintain expression of some AIRE-induced TRA (34). However, that we could detect only 2.8% (90 out of 3272) of AIRE-induced genes in the mTEC^{lo} subset casts some doubt on the biological role of post-AIRE cells in establishment of central tolerance to AIRE-dependent TRA. Nevertheless, we must not discount the possibility that post-AIRE cells may still present MHC–peptide complexes that have a long half-live and persist at the cell surface in the absence of the peptide (i.e., TRA) coding transcript.

AIRE-induced versus -independent TRA

Aire-KO mice certainly facilitate the identification of AIRE-dependent genes. However, definition of TRA, and in particular AIRE-independent TRA, is a more complex question. We adopted

the definition stipulating that TRA-coding genes are those that are tissue enriched (i.e., expressed at relatively high levels) in at most five tissues (35). To identify these genes, we used a comprehensive catalog of gene expression in various tissues of C57BL/6 mice (GSE10246) (36). We then had to select a relative expression threshold to define tissue enrichment. The impact of this criterion is illustrated for two canonical TRA (*Ins2* and *Crp*) (Supplemental Fig. 4A). When we adopt a stringent criterion for tissue enrichment (expression level in a given tissue of ≥1000-fold the median expression across all tissues), both *Ins2* and *Crp* qualify as TRA. However, when we use a less stringent threshold (≥10-fold), *Ins2* no longer qualifies as a TRA because it is then considered to be enriched in more than five tissues. Consistent with this, we found that the enrichment threshold could have a major influence on the number of TRA detected in mTEC^{hi}. Whereas the number of AIRE-induced TRA remained stable at different thresholds, the number of AIRE-independent TRA increased dramatically when lowering the stringency (Fig. 4C). We reasoned that if we wanted to analyze the characteristics of AIRE-independent TRA, it was preferable to favor robustness over sensitivity. We therefore selected the most stringent threshold (1000-fold) for further analyses.

First, we validated that our TRA list included known AIRE-induced and AIRE-independent TRA (Supplemental Fig. 4B). It has been shown that the degree of pGE conforms to the following hierarchy: mTEC^{hi} > mTEC^{lo} > cTEC (9, 18). We therefore validated the expression pattern of our TRA in TEC populations. Although AIRE-induced TRA were solely expressed in WT mTEC^{hi}, AIRE-independent TRA were predominantly expressed in mTEC^{hi}, but also detectable in mTEC^{lo} and cTEC (Supplemental Fig. 4C).

Using our list of TRA, we next assessed to what extent AIRE-induced versus AIRE-independent transcription contributes to the pool of TRA expressed in mTEC^{hi}. When considering genes with RPKM of >1, we found that out of the 1367 AIRE-induced genes, 343 (25%) encoded TRA. In contrast, 504 (3.7%) of the 13,709 AIRE-independent genes encoded TRA (Fig. 4D). Finally, only six genes fell into the AIRE-repressed category. Two points can be made from these data. First, most AIRE-induced genes are not TRA. Second, although AIRE-induced genes are enriched in TRA ($p < 2.2 \times 10^{-16}$), ~60% of total TRA detected in mTEC^{hi} were AIRE-independent.

Evidence suggests that AIRE plays a role in mRNA processing and contributes to the expression of tissue-specific isoforms in mTEC (37, 38). We therefore analyzed mRNA splicing in TEC population harvested from WT and KO mice (Supplemental Fig. 3D, 3E). We found that WT mTEC^{hi} had a higher splicing complexity than did KO mTEC^{hi} and other TEC populations, confirming AIRE's role in mRNA splicing. Furthermore, *Aire* deletion had no effect on the splicing complexity of mTEC^{lo} and cTEC. Then, we asked whether the pool of AIRE-independent TRA significantly contributes to the high splicing complexity observed in mTEC^{hi} (Fig. 4E). Notably, we found that the splicing complexity of AIRE-independent TRA was superior to that of AIRE-induced TRA. Interestingly, when comparing the expression of >400 mouse RNA-binding proteins uploaded from the database of RNA-binding specificities (RBPDB version 1.3.1) (39), we identified 7 genes implicated in mRNA processing and whose expression was at least 2-fold higher in mTEC^{hi} relative to mTEC^{lo} and cTEC (Fig. 4F). Taken together, these results suggest that apart from AIRE, other mRNA processing factors expressed in mTEC^{hi} contribute to the high splicing complexity found in this cell population.

Tissue representation by AIRE-induced and -independent TRA

AIRE controls the expression of self-antigens representing peripheral tissues and organs (10). In human, *AIRE* mutations impair clonal deletion of T cells and cause the autoimmune polyendocrinopathy–candidiasis–ectodermal dystrophy (APECED) syndrome (40). This syndrome exhibits pleiotropic manifestations affecting many organs (41, 42).

To define the set of tissues represented in TEC by AIRE-induced and AIRE-independent TRA, we calculated the number of TRA specific for each tissues of the GSE10246 dataset. Furthermore, we determined the tissue enrichment ratio (odds ratio) for AIRE-induced relative to AIRE-independent TRA (Fig. 5A). This approach allowed us to assess the level of overlap between tissues represented by the two classes of TRA. We found that tissues and organs preferentially represented by AIRE-induced TRA included typical organs affected in APECED patients (e.g., pancreas, adrenal gland, stomach, liver), with the exception of the parathyroid gland, which is not included in the GSE10246 dataset. Although we detected several AIRE-independent pancreatic TRA, most pancreas-specific TRA (77%) were AIRE induced (Fig. 5A). These include genes encoding pancreatic digestive enzymes such as the chymotrypsin-like elastase family of proteins (*Cel3b*, *Cela1*), lipases (*Pnlip*, *Pnliprp1*, *Pla2g1b*, *Cel*), proteases (*Prss1*, *Prss2*), and regenerating islet-derived proteins (*Reg1*, *Reg2*, *Reg3b*). Other tissues preferentially represented by AIRE-induced TRA include the lactating mammary gland, bone, white adipose tissue, placenta, lacrimal gland, bone marrow, retinal epithelium, salivary gland, uterus, and cornea (Fig. 5A). Unexpectedly, we found that several tissues targeted in APECED patients (e.g., epidermis, ovary, and pituitary gland) were predominantly represented by AIRE-independent TRA. Thus, among ovarian genes, *Hsd3b1* (biosynthesis of hormonal steroid) was AIRE induced whereas *Ovgp1* (oviductal epithelial glycoprotein), *Akr1cl* (progesterone metabolism), and *Inha* (gonadal hormone secretion) were AIRE-independent. Other tissues and cell populations preferentially represented by AIRE-independent TRA include macrophages, NK cells, B cells, amygdala, osteoblasts, skeletal muscle, spleen, prefrontal cerebral cortex, and testes (Fig. 5A).

When we combined the two types of TRA, we found that the tissues that were most represented by TRA were the liver, small and large intestine, stomach, testis, kidney, epidermis, pancreas, and placenta. Overall, we detected TRA (RPKM > 1) specific for >50 tissues and cell types in the transcriptome of mTEC^{hi}. However, we also identified tissues and cell types with low thymic representation, including hematopoietic stem cells, common myeloid progenitor, thymocytes, T cells, dendritic cells, mega-erythrocyte progenitors, granulocyte progenitors, microglia, iris, and ciliary bodies (data not shown).

Evidence suggests that pGE in TEC is regulated by epigenetic mechanisms that support a hyperactive transcriptional state (43). This can be exemplified with AIRE's ability to bind nonmethylated histone H3K4 to promote gene transcription (44, 45). However, epigenetic regulators of AIRE-independent pGE have not been identified. The genome of embryonic stem cells (ESCs) and testicular cells undergoes major chromatin alterations during development (46). Importantly, AIRE has also been detected in ESCs and spermatocytes (47–49). Interestingly, we observed that several ESC- and testis-specific TRA were expressed in mTEC^{hi} (Fig. 5A). For example, we detected TRA involved in embryonic development (*Tdgf1*) as well as in the maintenance of ESC pluripotency (*Pou5f1*, *Dppa5a*). Testis-specific AIRE-induced TRA include a germ cell–associated gene (*Gsg1*) and spermatogenesis-associated genes (*Spata18*, *Spata19*). For AIRE-independent TRA, we found genes encoding proteins involved in sperm DNA condensation (*Tnp2*, *Tssk6*), male meiosis (*Rsph1*), sperm function and fertility (*Meig1*, *Tcp11*, *Spa17*, *Ropn1l*, *Tssk3*, *Tekt2*), translation of germ cell mRNA (*Ybx2*), testis-specific H1 histone (*H1fnt*), and cancer-testis

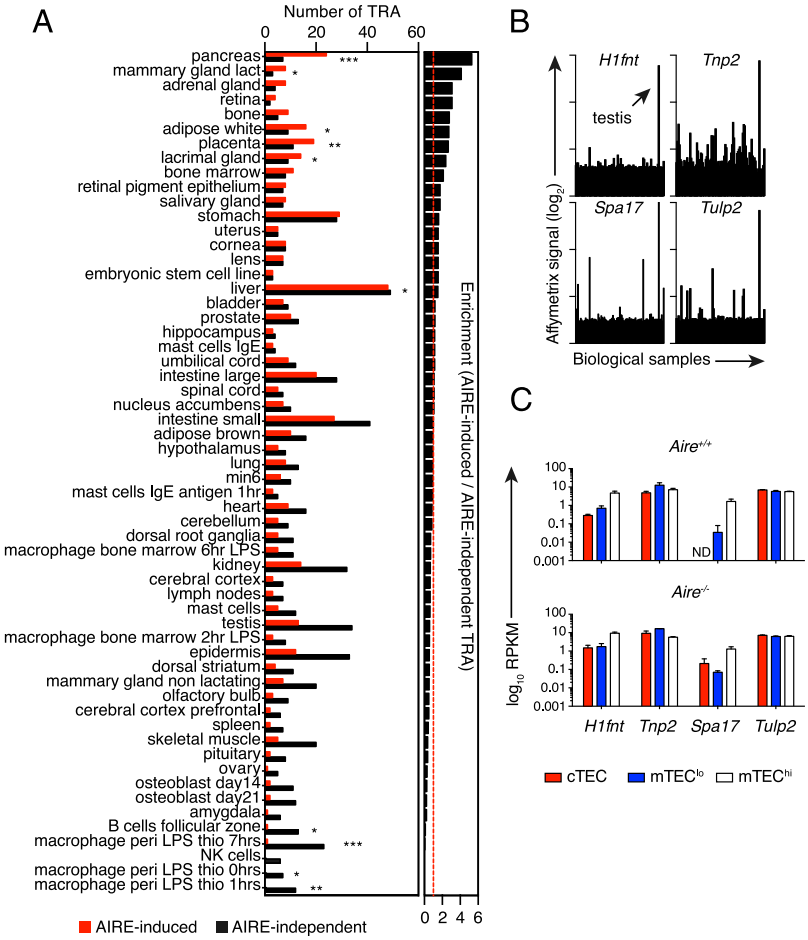

FIGURE 5. Peripheral tissue representation of AIRE-induced and AIRE-independent TRA. (**A**) Histogram depicting the number of AIRE-induced (red bars) and AIRE-independent TRA (black bars) representing mouse tissues and cell lines (GSE10246 dataset). Biological samples are ordered based on their differential representation by AIRE-induced and AIRE-independent TRA. Tissues that are represented by fewer than five TRA are not displayed on the histogram. A Fisher exact test was used to assess the enrichment in each sample. $*p < 0.05$, $**p < 0.01$, $***p < 0.001$. (**B**) Expression of testis-specific AIRE-independent TRA in tissues of the GSE10246 dataset (36) and in (**C**) TEC populations from WT and $Aire^{-/-}$ mice. Error bars indicate SD. ND, not detected.

Ags (*Tubl2*, *Rsph1*, *Prm1*). We speculate that these genes may be instrumental in regulating pGE in TEC. Overall, our data on TRA led us to conclude that defects in AIRE-independent pGE should cause severe autoimmune phenotypes because 1) AIRE-induced versus -independent TRA project nonredundant representations of peripheral tissues in the thymus, and 2) AIRE-independent TRA are more numerous than AIRE-induced TRA. Such autoimmune phenotype should be particularly conspicuous for organs, such as the testis, that are represented in TEC mostly by AIRE-independent TRA. Indeed, transcripts such as *H1fnt*, *Tnp2*, *Spa17*, and *Tulp2* have a very restricted tissue distribution in extrathymic tissues where they are expressed at higher levels in the testis than in other organs (Fig. 5B). In TEC, these testis TRA have an expression pattern that is typical of AIRE-independent TRA (Fig. 5C). We therefore propose that such testis TRA may represent the elusive T cell epitopes that initiate a common autoimmune disease: autoimmune orchitis. Male patients with autoimmune orchitis produce antisperm Abs, display severe sperm dysfunctions, and are infertile (50). This hypothesis might be evaluated by testing for T cell reactivity against testis TRA in subjects with autoimmune orchitis.

Biological processes regulated by promiscuously expressed genes

As shown in Fig. 4A, AIRE induces the expression of >3000 genes. Out of these genes, 1367 had RPKM > 1, of which only 343 (25%) were classified as TRA. Thus, the vast majority of AIRE-induced genes are not TRA. We hypothesized that this set of 1024 non-TRA AIRE-induced genes may be instrumental in AIRE's alternative functions. By alternative functions we mean functions distinct from TRA presentation by mTEC^{hi}, such as mTEC differentiation and mTEC interactions with thymocytes and DCs (15–17). To address this, we performed a GO term enrichment analysis on non-TRA AIRE-induced genes and we analyzed more extensively the top 10 enriched biological processes (Fig. 6A, 6B). The top GO term hit for our set of input genes was "cell adhesion." A heat map of genes implicated in the cell adhesion category (Fig. 6C) revealed that many key regulators of cell–cell interactions were upregulated in WT mTEC^{hi}: claudins (*Cldn11*, *Cldn15*), integrins (*Itgae*, *Itgam*, *Itgb2l*, *Itgad*), selectins (*Sele*, *Selp*), and extracellular matrix-associated molecules (*Hapln3*, *Lamc3*, *Thbs4*). Their upregulation in mTEC^{hi} could drastically enhance mTEC^{hi} homotypic interactions and explain why *Aire* deletion disturbs mTEC^{hi} distribution in the thymic medulla and prevents the formation of Hassall's corpuscle-like structures (15, 51). Likewise, differential expression of claudins, integrins, and selectins should have a significant impact on mTEC^{hi} heterotypic interactions with DCs and thymocytes (52, 53). The presence of Vanin-1 (*Vnn1*) in this category (RPKM of ~5) is also noteworthy because this GPI-anchored protein regulates the migration of hematopoietic T cell precursors to the thymus (54). The downregulation of *Vnn1* in *Aire*-KO mTEC^{hi} suggests that AIRE may promote homing of T cell progenitors to the thymus.

Consistent with a previous report (55), we found the "defense response" term to be enriched in our set of AIRE-induced genes. In addition to defensins (*Defa22*, *Defb3, 4, 19, 25, 50*), we identified several molecules involved in antiviral/antibacterial (*Ifnb1*, *Stab1*) immune responses, including ILs (*Il5, Il9*), chemokines (*Ccl1*, *Ccl20*, *Ccl28*, *Xcl1*), and antiviral enzymes (*Oas* gene

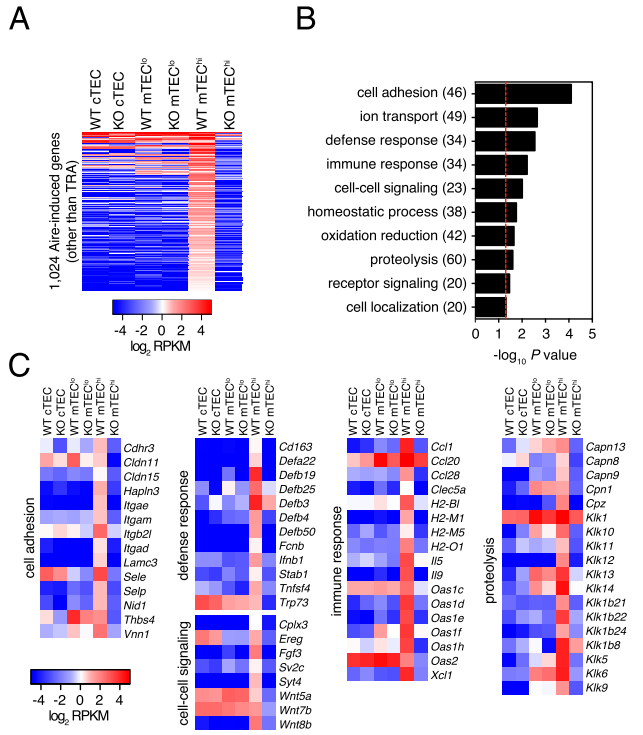

FIGURE 6. Biological processes associated to AIRE-induced promiscuously expressed genes. (**A**) Expression heat map of the 1024 AIRE-induced non-TRA encoding genes (input genes) in TEC populations. (**B**) GO term enrichment analysis on the set of input genes. Red dashed line represent $p = 0.05$. Numbers in parentheses indicate the number of genes per category. (**C**) Expression heat map of genes associated to the cell adhesion, defense response, immune response, cell–cell signaling, and proteolysis terms.

family). Notably, *Xcl1* and *Ccl20* regulate DC and thymocyte migration, respectively (56, 57). In accordance with the role of *Aire* in increasing antigenic presentation, we found that *Aire* upregulates the expression of *Tnfsf4*, which acts as a costimulator between thymocytes and APCs and thereby enhances the development of regulatory T cells (58).

Additionally, we found in the "cell–cell signaling" category several genes that could be highly relevant to TEC biology. For instance, in line with the peculiar ability of mTEC^{hi} to transfer cytoplasmic content to neighboring DCs (17), we found that *Aire* upregulates genes implicated in synaptic exocytosis (*Cplx3*, *Sv2c*) and vesicular trafficking (*Syt4*). However, whether mTEC use strategies similar to synaptic neurons to deliver the content of secretory vesicles remains an open field of investigation. Finally, in line with the role of WNT proteins in TEC biology (59), we found that three *Wnt* genes were upregulated in WT mTEC^{hi}.

The "proteolysis" term was also enriched in our set of input genes. Of note, we observed that *Aire* induced several proteases (*Cpln8*, *9*, *13*) and carboxypeptidases (*Cpn1*, *Cpz*). These enzymes could influence not only housekeeping functions, but also MHC Ag processing, which is instrumental in induction of central tolerance, the quintessential role of mTEC^{hi} (5).

Discussion

One conclusion emerging from this study is that AIRE decreases, via non–cell autonomous mechanisms, the number of cTEC by repressing positive regulators of cell differentiation and proliferation. As a parsimonious explanation for the effect of AIRE on cTEC, we surmise that it results from cell–cell signaling initiated by AIRE-regulated molecules secreted by mTEC or expressed at the surface of mTEC. Although the functional importance of this effect has yet to be demonstrated, we propose that it may contribute to the dramatic changes in TEC subsets that occur in the neonatal period: expansion of the mTEC compartment in the first weeks of life is accompanied by an abrupt decrease in the number of cTEC (19). Therefore, although cTEC are the dominant TEC subset at birth, they represent only 10% of TEC in adults (60). Moreover, we confirmed that the impact of AIRE-dependent pGE is not limited to generation of TRA. In fact, our results show that 75% of AIRE-induced genes are not TRA and are associated to several biologically relevant functions in mTEC. Previous reports have shown that, irrespective of its ability to generate TRA, AIRE enhances mTEC interactions with DCs and thymocytes. In line with this, we provide mechanistic explanations for these effects. Indeed, we found that AIRE-driven pGE upregulates the expression of numerous candidate genes that play a dominant role in cell–cell interactions: claudins, integrins, selectins, the costimulator TNFSF4, as well as genes mediating synaptic exocytosis and vesicular trafficking. Importantly, gain- and loss-of-function–based experiments will be required to 1) tie gene expression to biological functions and to 2) evaluate the role of these molecules in homotypic and heterotypic interactions involving mTEC^{hi} and their role in induction of central tolerance. The upregulation of proteases and peptidases by AIRE is also of prime interest. Indeed, the massive pGE observed in mTEC^{hi} must represent a challenge for proteostasis in these cells. Assuming that promiscuously expressed genes are translated, mTEC^{hi} must have to deal with high intracellular protein levels that would normally trigger proteotoxic stress response and proliferative exhaustion (61). There are only two ways to deal with this problem: by decreasing translation or increasing protein degradation. We therefore speculate that upregulation of proteases and peptidases may have an important role in alleviating proteotoxic stress in mTEC^{hi}.

pGE in TEC is essential to prevent autoimmunity. Although the fascinating mechanistic underpinnings of AIRE-dependent pGE are rather well understood, AIRE-independent pGE remains an enigma. Our report shows that AIRE-induced and -independent TRA present several distinctive features. First, we confirmed that AIRE-induced TRA are found exclusively in mTEC^{hi} whereas AIRE-independent TRA are detected not only in mTEC^{hi} but also in cTEC and mTEC^{lo} (9). Additionally, we show that relative to AIRE-induced TRA, AIRE-independent TRA 1) are more numerous and 2) show greater splicing complexity. Our observations on splicing complexity suggest that mRNA splicing factors overexpressed in mTEC^{hi} regulate the processing of AIRE-independent TRA for the generation of tissue-specific isoforms. We propose that particular attention should be paid to *Snrpn*, a modulator of alternative splicing (62) whose expression was 5-fold higher in mTEC^{hi} than in other TEC populations (GSE65617). Additionally, we observed that some tissues are represented in TEC mostly by AIRE-induced TRA whereas others are represented mainly by AIRE-independent TRA. Taken together, these data mean that AIRE-induced versus -independent pGE are not functionally redundant and that impairment of AIRE-independent pGE should lead to autoimmunity. Arguably the most perplexing question in this field is the identity of genes responsible for AIRE-independent pGE. In this regard, it is notable that AIRE-independent TRA were strikingly enriched in ovary- and testis-specific genes (Fig. 5A). This could be a meaningful clue as to the identity of AIRE-independent pGE regulators, because transcriptional regulation in germ cells is different from that in typical somatic cells. Germ cells have a unique chromatin reorganization program and use distinct promoter elements and transcription factors (63). We therefore hypothesize that germ cell–specific

transcriptional regulators that are promiscuously expressed in TEC may be responsible for AIRE-independent pGE.

Acknowledgments

We are grateful to Danièle Gagné and Gaël Dulude (flow cytometry and cell sorting), Marianne Arteau (RNA-seq experiment), and Patrick Gendron (bioinformatics) for help and sound advice. We also thank the personnel of the Institute for Research in Immunology and Cancer animal care facility.

Disclosures

The authors have no financial conflicts of interest.

References

1. Blais, M.-E., S. Brochu, M. Giroux, M.-P. Bélanger, G. Dulude, R.-P. Sékaly, and C. Perreault. 2008. Why T cells of thymic versus extrathymic origin are functionally different. *J. Immunol.* 180: 2299–2312.
2. Boehm, T., I. Hess, and J. B. Swann. 2012. Evolution of lymphoid tissues. *Trends Immunol.* 33: 315–321.
3. Suen, A. Y. W., and T. A. Baldwin. 2012. Proapoptotic protein Bim is differentially required during thymic clonal deletion to ubiquitous versus tissue-restricted antigens. *Proc. Natl. Acad. Sci. USA* 109: 893–898.
4. Cowan, J. E., S. M. Parnell, K. Nakamura, J. H. Caamano, P. J. L. Lane, E. J. Jenkinson, W. E. Jenkinson, and G. Anderson. 2013. The thymic medulla is required for Foxp3$^+$ regulatory but not conventional CD4$^+$ thymocyte development. *J. Exp. Med.* 210: 675–681.
5. Klein, L., B. Kyewski, P. M. Allen, and K. A. Hogquist. 2014. Positive and negative selection of the T cell repertoire: what thymocytes see (and don't see). *Nat. Rev. Immunol.* 14: 377–391.
6. Miller, F. W., L. Alfredsson, K. H. Costenbader, D. L. Kamen, L. M. Nelson, J. M. Norris, and A. J. De Roos. 2012. Epidemiology of environmental exposures and human autoimmune diseases: findings from a National Institute of Environmental Health Sciences Expert Panel Workshop. *J. Autoimmun.* 39: 259–271.
7. Klein, L., M. Hinterberger, G. Wirnsberger, and B. Kyewski. 2009. Antigen presentation in the thymus for positive selection and central tolerance induction. *Nat. Rev. Immunol.* 9: 833–844.
8. St-Pierre, C., S. Brochu, J. R. Vanegas, M. Dumont-Lagacé, S. Lemieux, and C. Perreault. 2013. Transcriptome sequencing of neonatal thymic epithelial cells. *Sci Rep* 3: 1860.
9. Sansom, S. N., N. Shikama-Dorn, S. Zhanybekova, G. Nusspaumer, I. C. Macaulay, M. E. Deadman, A. Heger, C. P. Ponting, and G. A. Holländer. 2014. Population and single-cell genomics reveal the Aire dependency, relief from Polycomb silencing, and distribution of self-antigen expression in thymic epithelia. *Genome Res.* 24: 1918–1931.
10. Liston, A., S. Lesage, J. Wilson, L. Peltonen, and C. C. Goodnow. 2003. Aire regulates negative selection of organ-specific T cells. *Nat. Immunol.* 4: 350–354.
11. Mathis, D., and C. Benoist. 2009. Aire. *Annu. Rev. Immunol.* 27: 287–312.
12. Danso-Abeam, D., K. A. Staats, D. Franckaert, L. Van Den Bosch, A. Liston, D. H. D. Gray, and J. Dooley. 2013. Aire mediates thymic expression and tolerance of pancreatic antigens via an unconventional transcriptional mechanism. *Eur. J. Immunol.* 43: 75–84.
13. Waterfield, M., I. S. Khan, J. T. Cortez, U. Fan, T. Metzger, A. Greer, K. Fasano, M. Martinez-Llordella, J. L. Pollack, D. J. Erle, et al. 2014. The transcriptional regulator Aire coopts the repressive ATF7ip-MBD1 complex for the induction of immunotolerance. *Nat. Immunol.* 15: 258–265.
14. Giraud, M., H. Yoshida, J. Abramson, P. B. Rahl, R. A. Young, D. Mathis, and C. Benoist. 2012. Aire unleashes stalled RNA polymerase to induce ectopic gene expression in thymic epithelial cells. *Proc. Natl. Acad. Sci. USA* 109: 535–540.
15. Yano, M., N. Kuroda, H. Han, M. Meguro-Horike, Y. Nishikawa, H. Kiyonari, K. Maemura, Y. Yanagawa, K. Obata, S. Takahashi, et al. 2008. Aire controls the differentiation program of thymic epithelial cells in the medulla for the establishment of self-tolerance. *J. Exp. Med.* 205: 2827–2838.
16. Anderson, M. S., E. S. Venanzi, Z. Chen, S. P. Berzins, C. Benoist, and D. Mathis. 2005. The cellular mechanism of Aire control of T cell tolerance. *Immunity* 23: 227–239.
17. Hubert, F.-X., S. A. Kinkel, G. M. Davey, B. Phipson, S. N. Mueller, A. Liston, A. I. Proietto, P. Z. Cannon, S. Forehan, G. K. Smyth, et al. 2011. Aire regulates the transfer of antigen from mTECs to dendritic cells for induction of thymic tolerance. *Blood* 118: 2462–2472.
18. Derbinski, J., J. Gäbler, B. Brors, S. Tierling, S. Jonnakuty, M. Hergenhahn, L. Peltonen, J. Walter, and B. Kyewski. 2005. Promiscuous gene expression in thymic epithelial cells is regulated at multiple levels. *J. Exp. Med.* 202: 33–45.
19. Gray, D. H. D., N. Seach, T. Ueno, M. K. Milton, A. Liston, A. M. Lew, C. C. Goodnow, and R. L. Boyd. 2006. Developmental kinetics, turnover, and stimulatory capacity of thymic epithelial cells. *Blood* 108: 3777–3785.
20. Wong, K., N. L. Lister, M. Barsanti, J. M. C. Lim, M. V. Hammett, D. M. Khong, C. Siatskas, D. H. D. Gray, R. L. Boyd, and A. P. Chidgey. 2014. Multilineage potential and self-renewal define an epithelial progenitor cell population in the adult thymus. *Cell Reports* 8: 1198–1209.
21. Anders, S., D. J. McCarthy, Y. Chen, M. Okoniewski, G. K. Smyth, W. Huber, and M. D. Robinson. 2013. Count-based differential expression analysis of RNA sequencing data using R and Bioconductor. *Nat. Protoc.* 8: 1765–1786.
22. Anders, S., and W. Huber. 2010. Differential expression analysis for sequence count data. *Genome Biol.* 11: R106.
23. Mortazavi, A., B. A. Williams, K. McCue, L. Schaeffer, and B. Wold. 2008. Mapping and quantifying mammalian transcriptomes by RNA-Seq. *Nat. Methods* 5: 621–628.
24. Huang, W., B. T. Sherman, and R. A. Lempicki. 2009. Systematic and integrative analysis of large gene lists using DAVID bioinformatics resources. *Nat. Protoc.* 4: 44–57.
25. Huang, W., B. T. Sherman, and R. A. Lempicki. 2009. Bioinformatics enrichment tools: paths toward the comprehensive functional analysis of large gene lists. *Nucleic Acids Res.* 37: 1–13.
26. Hubert, F.-X., S. A. Kinkel, K. E. Webster, P. Cannon, P. E. Crewther, A. I. Proeitto, L. Wu, W. R. Heath, and H. S. Scott. 2008. A specific anti-Aire antibody reveals aire expression is restricted to medullary thymic epithelial cells and not expressed in periphery. *J. Immunol.* 180: 3824–3832.
27. Cabral, A., P. Voskamp, A. M. Cleton-Jansen, A. South, D. Nizetic, and C. Backendorf. 2001. Structural organization and regulation of the small proline-rich family of cornified envelope precursors suggest a role in adaptive barrier function. *J. Biol. Chem.* 276: 19231–19237.
28. Vanhoutteghem, A., P. Djian, and H. Green. 2008. Ancient origin of the gene encoding involucrin, a precursor of the cross-linked envelope of epidermis and related epithelia. *Proc. Natl. Acad. Sci. USA* 105: 15481–15486.
29. Candi, E., R. Schmidt, and G. Melino. 2005. The cornified envelope: a model of cell death in the skin. *Nat. Rev. Mol. Cell Biol.* 6: 328–340.
30. Dudakov, J. A., A. M. Hanash, R. R. Jenq, L. F. Young, A. Ghosh, N. V. Singer, M. L. West, O. M. Smith, A. M. Holland, J. J. Tsai, et al. 2012. Interleukin-22 drives endogenous thymic regeneration in mice. *Science* 336: 91–95.
31. Jenkinson, W. E., E. J. Jenkinson, and G. Anderson. 2003. Differential requirement for mesenchyme in the proliferation and maturation of thymic epithelial progenitors. *J. Exp. Med.* 198: 325–332.
32. Villaseñor, J., W. Besse, C. Benoist, and D. Mathis. 2008. Ectopic expression of peripheral-tissue antigens in the thymic epithelium: probabilistic, monoallelic, misinitiated. *Proc. Natl. Acad. Sci. USA* 105: 15854–15859.
33. Derbinski, J., S. Pinto, S. Rösch, K. Hexel, and B. Kyewski. 2008. Promiscuous gene expression patterns in single medullary thymic epithelial cells argue for a stochastic mechanism. *Proc. Natl. Acad. Sci. USA* 105: 657–662.
34. Metzger, T. C., I. S. Khan, J. M. Gardner, M. L. Mouchess, K. P. Johannes, A. K. Krawisz, K. M. Skrzypczynska, and M. S. Anderson. 2013. Lineage tracing and cell ablation identify a post-Aire-expressing thymic epithelial cell population. *Cell Reports* 5: 166–179.
35. Pinto, S., C. Michel, H. Schmidt-Glenewinkel, N. Harder, K. Rohr, S. Wild, B. Brors, and B. Kyewski. 2013. Overlapping gene coexpression patterns in human medullary thymic epithelial cells generate self-antigen diversity. *Proc. Natl. Acad. Sci. USA* 110: E3497–E3505.
36. Lattin, J. E., K. Schroder, A. I. Su, J. R. Walker, J. Zhang, T. Wiltshire, K. Saijo, C. K. Glass, D. A. Hume, S. Kellie, and M. J. Sweet. 2008. Expression analysis of G protein-coupled receptors in mouse macrophages. *Immunome Res.* 4: 5.
37. Abramson, J., M. Giraud, C. Benoist, and D. Mathis. 2010. Aire's partners in the molecular control of immunological tolerance. *Cell* 140: 123–135.
38. Keane, P., R. Ceredig, and C. Seoighe. 2015. Promiscuous mRNA splicing under the control of AIRE in medullary thymic epithelial cells. *Bioinformatics* 31: 986–990.
39. Cook, K. B., H. Kazan, K. Zuberi, Q. Morris, and T. R. Hughes. 2011. RBPDB: a database of RNA-binding specificities. *Nucleic Acids Res.* 39: D301–D308.
40. Akirav, E. M., N. H. Ruddle, and K. C. Herold. 2011. The role of AIRE in human autoimmune disease. *Nat. Rev. Endocrinol.* 7: 25–33.
41. Villaseñor, J., C. Benoist, and D. Mathis. 2005. AIRE and APECED: molecular insights into an autoimmune disease. *Immunol. Rev.* 204: 156–164.
42. De Martino, L., D. Capalbo, N. Improda, F. D'Elia, R. Di Mase, R. D'Assante, I. D'Acunzo, C. Pignata, and M. Salerno. 2013. APECED: a paradigm of complex interactions between genetic background and susceptibility factors. *Front. Immunol.* 4: 331.
43. Tykocinski, L., A. Sinemus, E. Rezavandy, Y. Weiland, D. Baddeley, and C. Cremer. 2010. Epigenetic regulation of promiscuous gene expression in thymic medullary epithelial cells. *Proc. Natl. Acad. Sci. USA* 107: 19426–19431.
44. Org, T., F. Chignola, C. Hetényi, M. Gaetani, A. Rebane, I. Liiv, U. Maran, L. Mollica, M. J. Bottomley, G. Musco, and P. Peterson. 2008. The autoimmune regulator PHD finger binds to non-methylated histone H3K4 to activate gene expression. *EMBO Rep.* 9: 370–376.
45. Koh, A. S., A. J. Kuo, S. Y. Park, P. Cheung, J. Abramson, D. Bua, D. Carney, S. E. Shoelson, O. Gozani, R. E. Kingston, et al. 2008. Aire employs a histone-binding module to mediate immunological tolerance, linking chromatin regulation with organ-specific autoimmunity. *Proc. Natl. Acad. Sci. USA* 105: 15878–15883.
46. Reik, W. 2007. Stability and flexibility of epigenetic gene regulation in mammalian development. *Nature* 447: 425–432.
47. Nishikawa, Y., F. Hirota, M. Yano, H. Kitajima, J. Miyazaki, H. Kawamoto, Y. Mouri, and M. Matsumoto. 2010. Biphasic Aire expression in early embryos and in medullary thymic epithelial cells before end-stage terminal differentiation. *J. Exp. Med.* 207: 963–971.
48. Gu, B., J. Zhang, Q. Chen, B. Tao, W. Wang, Y. Zhou, L. Chen, Y. Liu, and M. Zhang. 2010. Aire regulates the expression of differentiation-associated genes and self-renewal of embryonic stem cells. *Biochem. Biophys. Res. Commun.* 394: 418–423.

49. Schaller, C. E., C. L. Wang, G. Beck-Engeser, L. Goss, H. S. Scott, M. S. Anderson, and M. Wabl. 2008. Expression of Aire and the early wave of apoptosis in spermatogenesis. *J. Immunol.* 180: 1338–1343.
50. Silva, C. A., M. Cocuzza, J. F. Carvalho, and E. Bonfá. 2014. Diagnosis and classification of autoimmune orchitis. *Autoimmun. Rev.* 13: 431–434.
51. Dooley, J., M. Erickson, and A. G. Farr. 2008. Alterations of the medullary epithelial compartment in the Aire-deficient thymus: implications for programs of thymic epithelial differentiation. *J. Immunol.* 181: 5225–5232.
52. Heiskala, M., P. A. Peterson, and Y. Yang. 2001. The roles of claudin superfamily proteins in paracellular transport. *Traffic* 2: 93–98.
53. Love, P. E., and A. Bhandoola. 2011. Signal integration and crosstalk during thymocyte migration and emigration. *Nat. Rev. Immunol.* 11: 469–477.
54. Aurrand-Lions, M., F. Galland, H. Bazin, V. M. Zakharyev, B. A. Imhof, and P. Naquet. 1996. Vanin-1, a novel GPI-linked perivascular molecule involved in thymus homing. *Immunity* 5: 391–405.
55. Ki, S., D. Park, H. J. Selden, J. Seita, H. Chung, J. Kim, V. R. Iyer, and L. I. R. Ehrlich. 2014. Global transcriptional profiling reveals distinct functions of thymic stromal subsets and age-related changes during thymic involution. *Cell Reports* 9: 402–415.
56. Bunting, M. D., I. Comerford, E. E. Kara, H. Korner, and S. R. McColl. 2014. CCR6 supports migration and differentiation of a subset of DN1 early thymocyte progenitors but is not required for thymic nTreg development. *Immunol. Cell Biol.* 92: 489–498.
57. Lei, Y., A. M. Ripen, N. Ishimaru, I. Ohigashi, T. Nagasawa, L. T. Jeker, M. R. Bösl, G. A. Holländer, Y. Hayashi, Rde. W. Malefyt, et al. 2011. Aire-dependent production of XCL1 mediates medullary accumulation of thymic dendritic cells and contributes to regulatory T cell development. *J. Exp. Med.* 208: 383–394.
58. Mahmud, S. A., L. S. Manlove, H. M. Schmitz, Y. Xing, Y. Wang, D. L. Owen, J. M. Schenkel, J. S. Boomer, J. M. Green, H. Yagita, et al. 2014. Costimulation via the tumor-necrosis factor receptor superfamily couples TCR signal strength to the thymic differentiation of regulatory T cells. *Nat. Immunol.* 15: 473–481.
59. Heinonen, K. M., J. R. Vanegas, S. Brochu, J. Shan, S. J. Vainio, and C. Perreault. 2011. Wnt4 regulates thymic cellularity through the expansion of thymic epithelial cells and early thymic progenitors. *Blood* 118: 5163–5173.
60. Dumont-Lagacé, M., S. Brochu, C. St-Pierre, and C. Perreault. 2014. Adult thymic epithelium contains nonsenescent label-retaining cells. *J. Immunol.* 192: 2219–2226.
61. Buszczak, M., R. A. J. Signer, and S. J. Morrison. 2014. Cellular differences in protein synthesis regulate tissue homeostasis. *Cell* 159: 242–251.
62. Lee, M. S., Y. S. Lin, Y. F. Deng, W. T. Hsu, C. C. Shen, Y. H. Cheng, Y. T. Huang, and C. Li. 2014. Modulation of alternative splicing by expression of small nuclear ribonucleoprotein polypeptide N. *FEBS J.* 281: 5194–5207.
63. Sassone-Corsi, P. 2002. Unique chromatin remodeling and transcriptional regulation in spermatogenesis. *Science* 296: 2176–2178.